Effects of Annealing on Morphology of Polymer/Polymer (PS/PMMA) Blend; a Fluorescence Study

Şaziye Uğur,[1] Önder Pekcan[2]

[1]*Istanbul Technical University, Department of Physics, 34469 Maslak, Istanbul, Turkey*
[2]*Isik University, Department of Physics, 34398 Maslak, Istanbul, Turkey*

Received 17 December 2004; accepted 27 June 2005
DOI 10.1002/app.23458
Published online in Wiley InterScience (www.interscience.wiley.com).

ABSTRACT: Steady state fluorescence (SSF) technique conjunction with optical microscopy were used to study the morphology of polystyrene (PS)/poly(methyl methacrylate) (PMMA) blend upon annealing above glass transition in elevated time intervals. The PS/PMMA blends were prepared from dissolution of pyrene (P) and naphthalene (N) labeled PS and PMMA particles, respectively. Monte Carlo simulations were performed to model the N and P fluorescence intensities (I_N and I_P), using photon diffusion theory. Number of N and P photons (N_N and N_P) emerging from the front surface of the blend are calculated when only N is excited, where N_P photons are combined of photons from radiative (N_{PR}) and nonradiative (N_{PNR}) energy transfer processes. Optical microscopy images were taken at each annealing step to support our findings from fluorescence measurements. © 2006 Wiley Periodicals, Inc. J Appl Polym Sci 100: 2104–2110, 2006

Key words: blend; fluorescence; annealing; energy transfer; optical microscopy

INTRODUCTION

Polymer coatings are of great technological interest. In addition to the application of pure polymers as protective layers, mixtures of two or more polymers called polymer blends can be used for coating industry. Blending of two or more thermoplastics may generate new materials, with a combination of properties that can not be found in pure polymers. For example, polystyrene (PS) and poly(methyl methacrylate) (PMMA) are immiscible in the whole composition range[1] and combination of PS and PMMA can be used to prepare an antireflection coating for glass.[2]

The property of a polymer strictly depends on its morphology. Therefore, understanding blend morphology is crucial during polymer processing. Most polymers are immiscible and produce multiphase blends. These blends combine characteristics of both constituent polymers in a manner that is related to the blend morphology. The morphology of the blend develops during annealing in a very complex way. Under the appropriate conditions, morphological structures such as spheres, ellipsoids, fibers, and plates or ribbon can be produced.

The surface morphology and composition of the solvent-cast blends of incompatible polymers can be modified by different factors such as casting solvent,[3] temperature,[4] and chain end groups.[5] Solvent-cast blends from volatile solution, such as chloroform or toluene, may not be thermodynamically equilibrated due to rapid solvent evaporation during the spin-casting process.[6] The solvent effects may be removed, or at least reduced, by annealing the cast films under appropriate conditions. Some authors have shown the effects of annealing on the surface composition of blends and block copolymers.[7,8] The surface analysis of PS/PMMA blends spin-cast from chloroform solution have been studied using X-ray photoelectron spectroscopy (XPS).[9]

The morphology of immiscible polymer blends shows a diversity with discrete and bi-continuous phase structures. In two phase blends with bi-continuous phase structure, both components form phases that partly or fully form a continuous phase, which present interpenetrating morphology through the whole volume of the sample.[10] The transition from discrete to bi-continuous phase structure is quite important in the sense that bi-continuous phase structure represents an infinite structure for an infinitely large sample. The effect of blend composition, phase viscosity, interfacial tension, and flow type on blend morphology have been extensively studied by different groups.[11–14]

Using time-resolved fluorescence (TRF) measurements in conjunction with dye-labeled particles, interdiffusion during latex film formation has been studied by Winnik and coworkers.[15–18] Direct nonradiative energy transfer (DET) method was employed to investigate the film formation processes in dye-labeled PMMA[12,18] and PBMA[16,17] systems. The steady state fluorescence (SSF) technique combined with DET has

Correspondence to: O. Pekcan (pekcan@isikun.edu.tr).

been used to examine healing and interdiffusion processes in dye-labeled PMMA latex films.[19–21] More recently, photon transmission[22,23] and fluorescence techniques were employed to investigate film formation from dye labeled latex particles.

Because of photon diffusion, radiative and nonradiative energy transfer processes, special attention has to be paid during SSF measurements to study the evolution of film formation. Film thickness and annealing time intervals are very critical for the quality of the film. In that sense, photon diffusion, radiative and nonradiative processes compete and may play important role during SSF measurements.[24] In this work, SSF measurements were performed to study changes in morphology of PS/PMMA blend by using DET method and optical microscopy. The PMMA and PS particles prepared by dispersion and emulsion polymerization were dissolved in chloroform. This solution was then used to cast the polymer/polymer blend on a glass plate. PMMA and PS particles were labeled with naphthalene (N) and pyrene (P) chromophores, respectively.[25,26]

In this paper, two sets of isothermal experiments were performed by annealing PS/PMMA blend samples at 180°C, in 20 min time intervals. In the first set; after annealing, only pyrene was excited at 345 nm and emission intensity (I_{0P}) was observed versus annealing time. This set of experiments was performed to detect the evolution of the quality (transparency) of the blend sample. During the second set of experiments, after annealing the blend sample, N and P intensities (I_N and I_P) were monitored against the annealing time, when the films were excited at 286 nm. In this set of experiments, we aimed to observe the DET across the polymer/polymer junction. Monte Carlo simulations were carried out to model the I_{0P}, I_N, and I_P intensities emitted from blend, using photon diffusion theory.

EXPERIMENTAL

Naphthalene (N) and pyrene (P) labeled PMMA and PS particles were produced separately via dispersion[25] and emulsion[26] polymerization, respectively. Blend preparation was carried out thus; the same weights (50% + 50%) of PMMA and PS particles were dissolved in chloroform in a test tube; after complete dissolution, a large drop of the solution was placed on a 1.5 × 1.5 cm^2 glass plate. After spin coating (500 rpm), chloroform was allowed to evaporate and the glass plate placed in the solid surface accessory of model LS-50 fluorescence spectrometer of Perkin-Elmer. All measurements were carried out in the front face position at room temperature. Slit widths were kept at 8 nm. The PS/PMMA blend sample was excited at 286 nm to maximize naphthalene absorbance while minimizing pyrene absorbance. Blend sample was illuminated only during the actual fluorescence measurements and, at all other times, were shielded from the light source. The blend was annealed above T_g of PMMA and PS for 20 min periods of time at 180°C. The temperature was maintained within ±2°C during annealing. The variation in optical density of the blend was monitored by Olympus BHSP Polarization microscope.

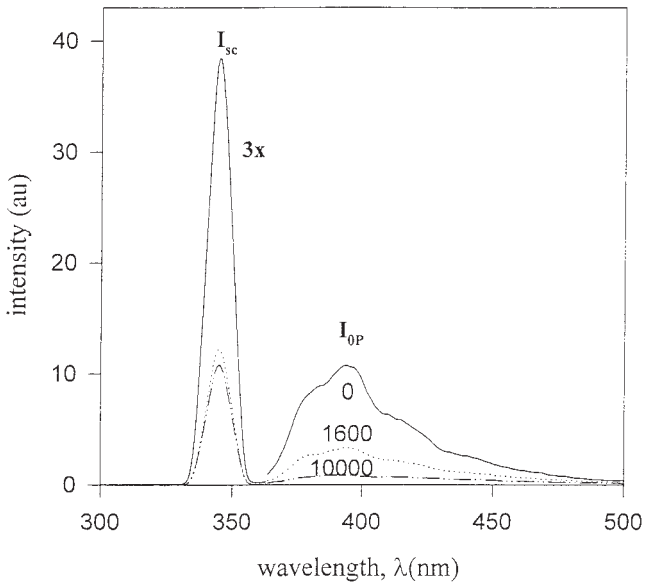

Figure 1 Pyrene emission (I_{0P}) and scattered (I_{sc}) spectra of PS/PMMA blend before annealing and after annealed at 180°C in 0, 1600, and 10,000 min time intervals. Blend is excited at 345 nm.

RESULTS AND DISCUSSION

Photon diffusion in PS/PMMA blend

Typical emission (I_{0P}) and scattered (I_{sc}) spectra from PS/PMMA blend annealed at 180°C in elevated time intervals and excited at 345 nm, are shown in Figure 1. Upon annealing, P intensity (I_{0P}) and I_{sc} decreased continuously from the beginning by increasing annealing time. The behavior of (I_{0P}) and (I_{sc}) versus annealing time are plotted in Figure 2(a) and 2(b), respectively. The variation in I_{0P} depends on optical path, *s*, of a photon in the blend. This optical path is directly proportional to the probability of a photon encountering a pyrene molecule. Before annealing, the photon is scattered from the particle surfaces, the mean free path, $<r>$ is of the order of the size of the PS, and PMMA domains, and after a few steps, it reemerges from the front surface of the film. Thus, the optical path, *s*, is long. Scattering is predominantly from the polymer/polymer interfaces and the mean free path becomes of the order of the domain size. Clearly, in this regime, with the same number of rescatterings, a photon will spend some time in the

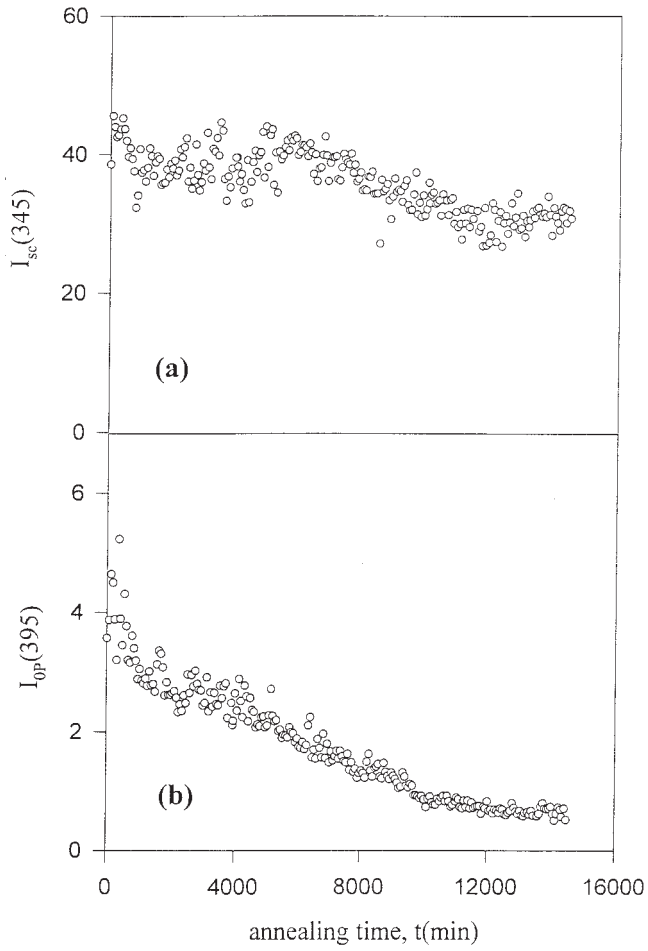

Figure 2 Variation of a- (I_{0P}) and (I_{sc}), intensities versus annealing time.

blend, and consequently, I_{0P}, values are large. Because of further annealing, the blend start to become essentially transparent to the photon, the mean free path diverges, and *s* eventually becomes of the order of the blend thickness, *d*. We have demonstrated, by means of Monte Carlo simulations to be discussed later that merely the blend represents a much shorter value for the optical path than that obtained by multiple scattering from interfaces. Hence, the decrease in I_{0P} after complete annealing has occurred.

The behavior of I_{0P} and I_{sc} can be interpreted by results of Monte Carlo simulations.[24] N_{0P} and N_{sc} are plotted versus square of mean free path ($<r>^2$) of a photon in Figure 3(a) and 3(b), respectively. When the annealing time increases, square of the mean free path increases. In Figure 3(a), N_{0P} decreases by increasing $<r>^2$ These indicate that for very short $<r>^2$ values, *s* is short but as $<r>^2$ values increase the optical path, *s* of a photon becomes longest and the probability of encountering a pyrene in the film is highest, as a result, N_{0P} is large. However, for longer $<r>^2$ values *s* becomes shorter and photons can easily escape from the back surface of the blend and both N_{0P} and N_{sc} decrease continuously by increasing $<r>^2$ values.

Optical micrographs

To support these findings, optical micrographs of the blend were taken, before and after annealing above T_g at elevated time intervals and presented in Figure 4. Figure 4 presents optical micrograph (OM) images of PS–PMMA blend film at different stages of annealing. Surface of the blend in Figure 4(a) shows many large irregular islands and few small spots between islands. These islands are divided into smaller islands and spots after annealing of the blend for 5000 min at 180°C as presented in Figure 4(b). Because of further annealing of the blend at 180°C small islands recombine and create larger islands as presented in Figure 4(c), where many small spots are shown both in the islands and between islands. To distinguish between PS and PMMA phases, blend in Figure 4(c) is treated with acetic acid to remove the PMMA. Figure 4(d) shows the inverted topographic contrast instead of islands. From here we conclude that islands consist of PMMA at the beginning and the end of the annealing. In Figure 4(d), small spots in the islands consist of PS, however small dots between islands are PMMA.

The blend in Figure 4(a) presents highest I_{0P}, however, the blend in Figure 4(b) gives the lower I_{0P} value. The corresponding I_{sc} intensities of film samples in Figure 4 show a decrease by increasing annealing time intervals. Micrograph results are found to be consis-

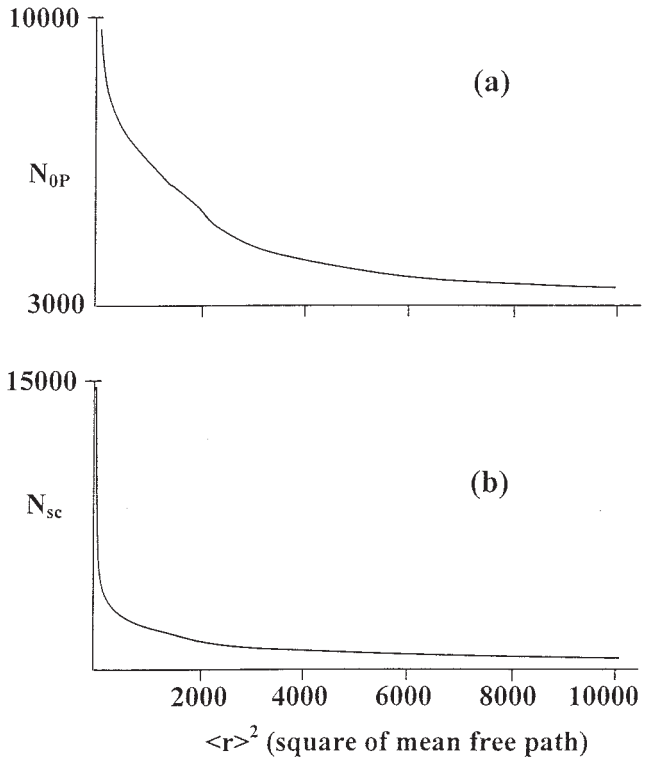

Figure 3 Variation of a- (N_{0P}) and (N_{sc}), versus, square of mean free path of a photon, $<r>^2$. Results are obtained from Monte Carlo simulations.

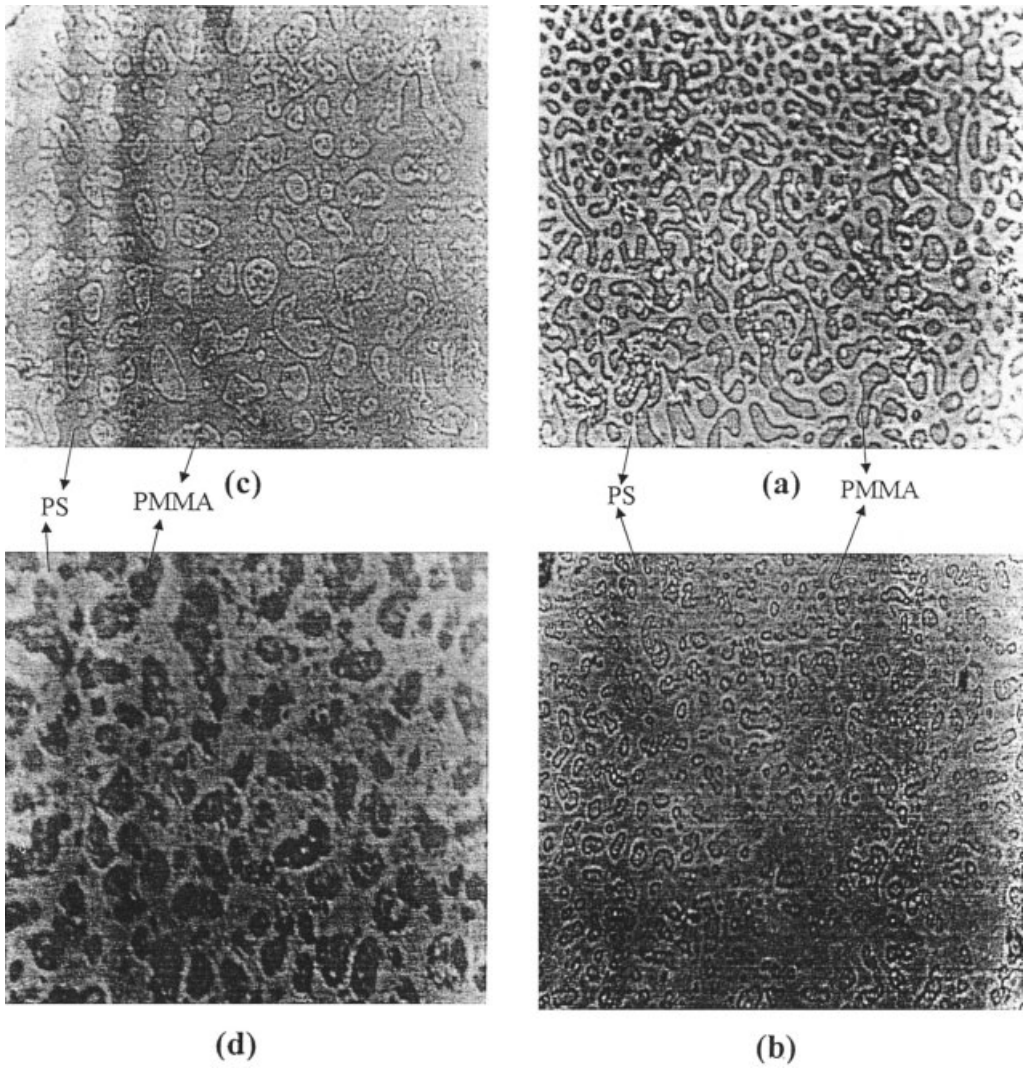

Figure 4 Micrographs of PS/PMMA blend (a) before annealing, (b) annealed at 180°C for 500 min, (c) annealed at 180°C for 8500 min time intervals and (d) after treated with acetic acid.

tent with the photon diffusion model. Cartoon representation and its relation with the mean free paths ($<r>$) are presented in Figure 5. Early stage of blend formation is shown in Figure 5(a), where high I_{0P} and I_{sc} values were observed because of very short $<r>^2$ values. Figure 5(b) presents a blend where, because of annealing, smaller islands are obtained that gives rise to short $<r>^2$ values. In this blend, one can observe lower I_{0P} and I_{sc} intensities. Finally, Figure 5(c) shows a semi transparent blend with the longest $<r>^2$ values. This film naturally presents both lowest I_{0P} and I_{sc} intensities.

Energy transfer processes in PS/PMMA blend

When the annealing process proceeds, domain boundaries disappear and DET between N and P molecules takes place. This picture can be quantitatively modeled by the results of Monte Carlo simulations.[24] The total number of P and N photons (N_P and N_N) emitted from the front surface of the blend are plotted versus $<r>^2$ of a photon in Figure 6(a) and 6(b), respectively, where N_P and N_N both decrease by increasing $<r>^2$. Since annealing time, t increases, $<r>^2$ also increases, then one should expect an increase in P and decrease in N intensities due to energy transfer from N to P molecules. Since, N_P contains photons from both radiative and nonradiative processes, earlier mentioned contradiction can be resolved using Monte Carlo simulations.[24] Figure 7(a) and 7(b) present the plot of N_{PR} and N_{PNR} versus $<r>^{2,}$ where one can observe continuous increase in N_{PNR} photons due to nonradiative energy transfer process from N to P molecules. Number of photons, because of radiative energy transfer (N_{PR}) process present very high values at the beginning of film formation, then decrease immediately because of increase in $<r>$ values. Now, Figure 6(b) and 7(b) look consistent by showing decrease in N

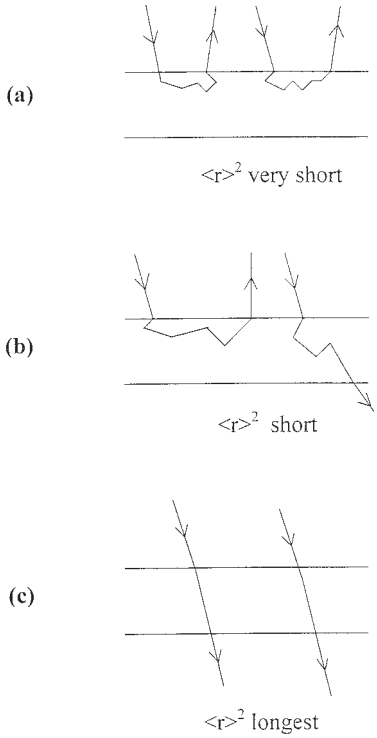

Figure 5 Cartoon representation of photon diffusion in PS/PMMA blend (a) before annealing, annealed at (b) short and (c) longer times.

photons and increase in P photons, respectively, but still this correspondence is not one to one. Here, emission from naphthalene, because of variation in blend quality (N_{0P}), dominates the total N_N emission. This contribution can be rationalized by comparing Figures

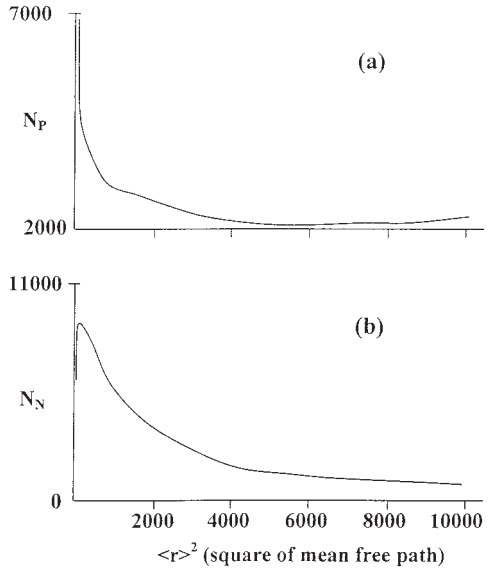

Figure 6 Variation of total number of (a) P (N_P) and (b) N (N_N) photons versus $<r>^2$, square of mean free path of a photon. Result is obtained from Monte Carlo simulations.[26]

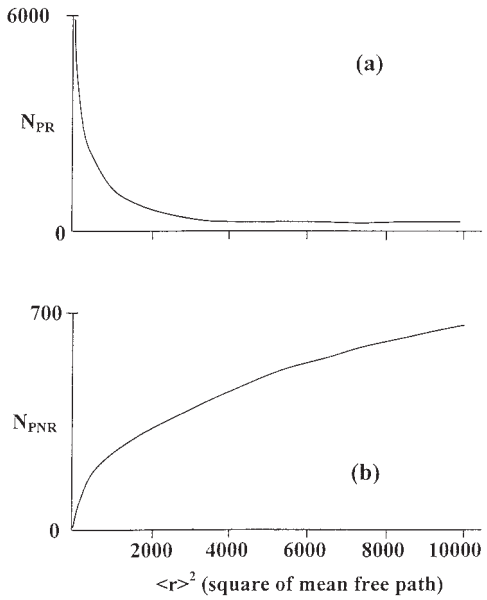

Figure 7 Variation of number of (a) P photons (N_{PR}) due to radiative transfer, (b) P photons (N_{PNR}) due to nonradiative transfer from N to P molecules, emitted from the front surface of the blend.

5(a) and 6(b) where the quality of the film (or $<r>$) affects the number of emitted photons in both case. To eliminate the photons (N_{0P}) created because of the variation in the quality of the film and to separate the contributions solely from the radiative and nonradiative energy transfer processes, we normalize the total number of photons emitted from the front surface of the film as follows

$$N_P' + N_N' = 100 \tag{1}$$

where, N_P' and N_N' are the total normalized number of P and N photons emitted from the front surface of the film, respectively. N_P' and N_N' are plotted versus $<r>^2$ of a photon in Figure 8(a) and 8(b), respectively, in which one to one correspondence between P and N emissions now can be seen. When Figure 7(b) is compared with Figure 8(a), it is seen that N_P' is created by nonradiative energy transfer process (N_{PNR}) except at very early N_{PR} contribution. The normalized photon emission from naphthalene N_N' now decreases due to nonradiative energy transfer from N to P as the mean free path $<r>$ of a photon increase, expect at the early stage, radiative energy transfer contribution.

The emission spectra of N and P labeled PS/PMMA blend before and after annealed at 180°C for 0, 1600, and total 10,000 min time intervals are shown in Figure 9, where the blend is excited at 286 nm. I_P and I_N are both decrease continuously by increasing annealing time intervals. The variation in I_P and I_N intensities versus annealing time are shown in Figure 10(a) and 10(b), respectively. From the point of view of DET, the

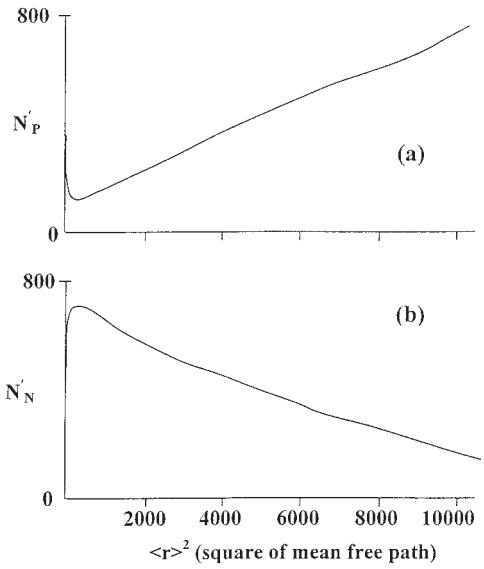

Figure 8 Variation of normalized total number of (a) P (N_P') and (b) N (N_N') photons versus, square of mean free path of a photon, $<r>^2$. Normalization is done according to eq. (1).

decrease in I_N is expected, but the decrease in I_P is quite surprising. One would naturally expect an increase in I_P due to DET processes as I_N decrease. In previous paragraph, Monte Carlo simulations have predicted that this anomalous behavior in I_P is produced due to the variation in the quality of the blend, which can be resolved by using eq. (1). The emission due to the variation in optical quality of the film can be eliminated by normalizing the total P and N intensities to 100. The variation in normalized P and N intensities (I_P' and I_N') versus annealing time are presented in Figure 11(a) and 11(b), respectively. As expected from Monte Carlo simulations, now as I_P'

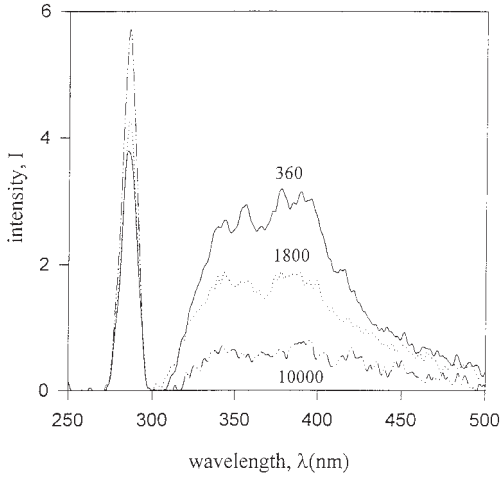

Figure 9 Emission (I_N and I_P) spectra of PS/PMMA blend before and after annealed at 0, 1600, min and 10,000 min time intervals at 180°C. Blend is excited at 286 nm.

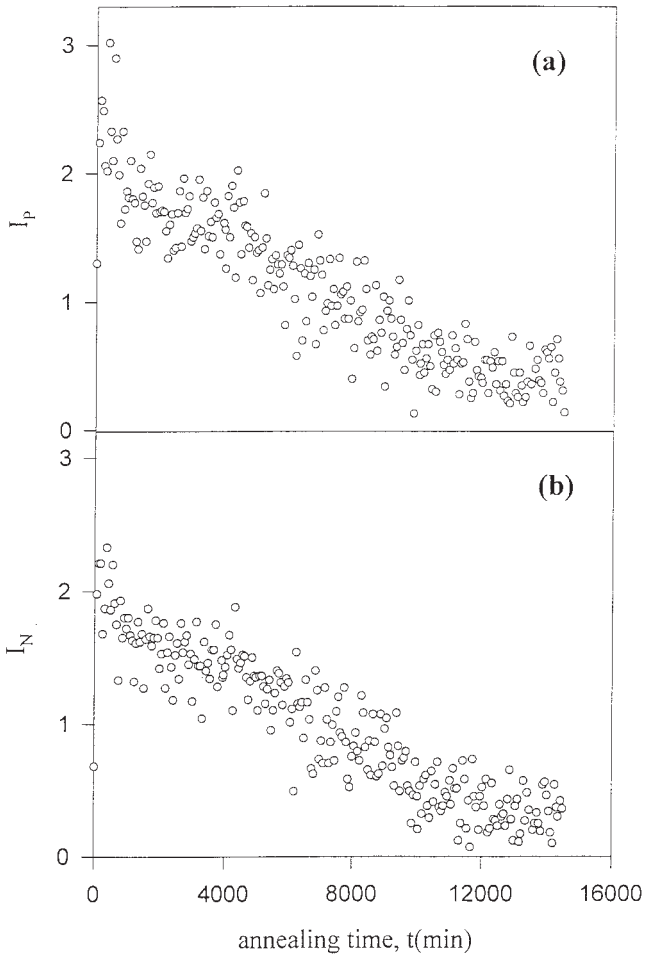

Figure 10 Variation of (a) P (I_P) and (b) N (I_N) intensities versus annealing time.

increase I_N' decreases by increasing annealing time. This behavior in I_P' and I_N' intensities show one to one correspondence, which indicates that the energy transfer processes between N and P are purely radiative and nonradiative.

This behavior of DET is consistent with the results of optical micrographs as shown in Figure 4. At the beginning, before annealing, naphthalenes are confined in PMMA islands and no energy transfer can be observed with pyrenes in PS background. However, annealing of blend for 5000 min at 180°C, because of the creation of small PMMA island and spots, DET starts to increase between N and P dyes. Further annealing at 180°C for 8500 min creates larger PMMA islands with PS dots and PMMA spots in PS background in the blend, which present high DET from N to P molecules as shown in Figure 11.

In conclusion, this work has shown that fluorescence technique conjunction with optical microscopy can be used to study morphological changes in polymer/polymer blend during annealing processes. This work can be extended for studying polymeric blends in various compositions and in different immiscible mixtures.

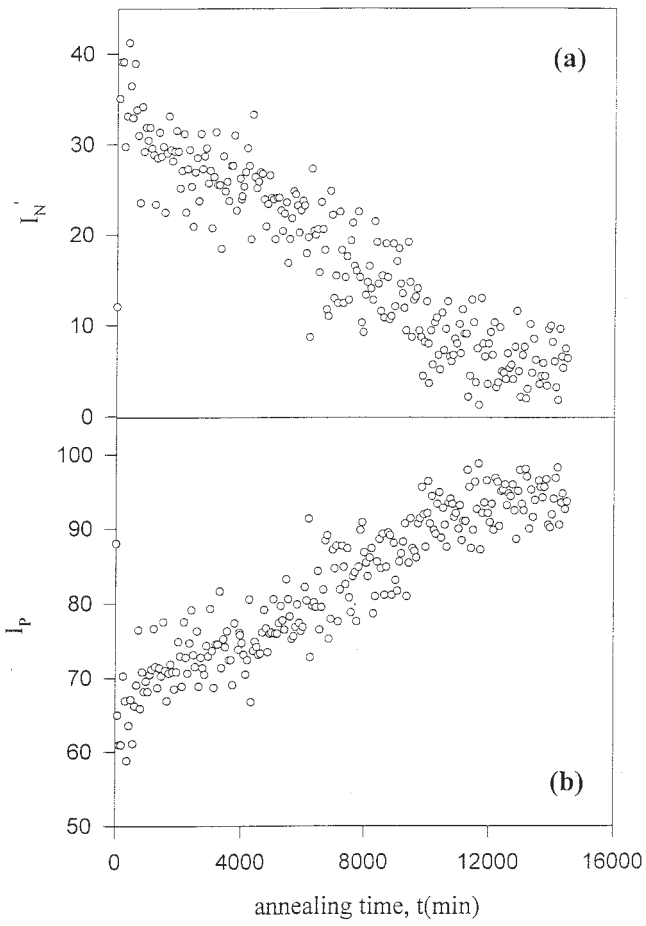

Figure 11 Variation of normalized (a) P (I_P') and (b) N (I_N') intensities versus annealing time. Normalization is performed using eq. (1).

References

1. Chaudhury, M. K. Mater Sci Eng 1996, 16, 97.
2. Walheim, S.; Schöffer, E.; Mlgnek, J; Steiner, U. Science 1999, 283, 520.
3. Scmidt, J. J.; Gardella, J. A.; Salvati, L. Macromolecules 1989, 22, 4489.
4. Lim, D. S.; Kyu, T. J Chem Phys 1990, 92, 3944.
5. Kajiyama, T.; Tanaka, K.; Takahara, A. Macromolecules 1998, 31, 3746.
6. Green, P. F.; Christensen, T. M.; Russel, T. P.; Jerome, R. J Chem Phys 1990, 92, 1478.
7. Chen, X.; Lee, H. L.; Gardella, J. A. Macromolecules 1993, 26, 4601.
8. Limary, R.; Green, P. F. Macromolecules 1999, 32, 8167.
9. Ton-That, C.; Shard, A. G.; Teare, D. O. H.; Bradley, R. H. Polymer 2000, 42, 1121.
10. Jorgensen, J. L.; Rasmussen, K. L.; Chtcherbakova, E. A.; Utracki, L. A. Polym Eng Sci 1999, 39, 1060.
11. Grace, H. P. Chem Eng Commu 1982, 14, 255.
12. Elmendrop, J. J.; Maatcke, R. J Polym Eng Sci 1985, 25, 1041.
13. Favis, B. D. Can J Chem Eng 1991, 69, 619.
14. Utracki, L. A.; Shi, Z. H. Polym Eng Sci 1992 32, 1827.
15. Pekcan, Ö.; Winnik, M. A.; Croucher, M. D. Macromolecules 1990, 23, 2673.
16. Wang, Y.; Zhao C. L.; Winnik, M. A. J Chem Phys 1991, 95, 2143.
17. Wang Y.; Winnik, M. A. J Phys Chem 1993, 97, 2507.
18. Wang, Y.; Winnik, M. A. Macromolecules 1993, 26, 3147.
19. Pekcan, Ö.; Canpolat, M.; Göçmen, A. Eur Polym Mater 1993, 29, 115.
20. Pekcan, Ö.; Canpolat, M.; Göçmen, A. Polymer 1993, 34, 3319.
21. Canpolat, M.; Pekcan, Ö. Polymer 1995, 36 2025.
22. Arda, E.; Özer, F.; Pi°kin, E.; Pekcan, Ö. J Coll Interface Sci 2001, 233, 271.
23. Arda, E.; Pekcan, Ö. Polymer 2001, 42, 7419.
24. Canpolat, M.; Pekcan, Ö. Polymer, 1997, 38, 2595.
25. Winnik, M. A.; Hua, M. H.; Hongham, B.; Williamson, B.; Croucher, M. D. Macromolecules 1984, 17, 262.
26. Uğur, Ş.; Elaissari, A.; Pekcan, Ö. J Coll Interface Sci 2003, 263, 674.